THE ASTROPHYSICAL JOURNAL, 342:666–676, 1989 July 15

Hα EMISSION LINES IN HIGH-REDSHIFT QUASARS

B. R. ESPEY AND R. F. CARSWELL
Institute of Astronomy, Cambridge
J. A. BAILEY
Anglo-Australian Observatory
M. G. SMITH
Joint Astronomy Centre
AND
M. J. WARD
University of Washington and Institute of Astronomy, Cambridge
Received 1988 September 28; accepted 1988 December 29

ABSTRACT

We have obtained, using the FIGS spectrometer at the Anglo-Australian Telescope, infrared spectra of the Hα lines in 18 medium- to high-redshift QSOs and optical spectra taken nearly simultaneously to measure the strong ultraviolet lines. We find that the Hα line is redshifted by an average of 1000 km s^{-1} with respect to the lines from high ionization species such as C IV. Low ionization lines, from ions such as O I and Mg II, are shifted by similar, or slightly smaller, amounts with respect to the high ionization lines. These results are difficult to reconcile with any simple models currently available, including those where dust obscuration is solely responsible for the observed velocity shifts. The similarity between the velocities of Hα and Mg II, O I provides some support for models in which the Balmer lines are produced predominantly in a warm H I region, perhaps by X-ray heating, while the Lyman lines arise mainly in a population of optically thin clouds. A velocity separation between the two cloud populations, along with some obscuration, could explain the main features. However, detailed differences between lines of similar ionization suggest that the true situation is more complex.

A search for correlations between the velocity shift and other parameters revealed only one, with the ratio of the C III] 1909 (Å) to C IV 1549 line fluxes. The meaning of this is obscure, but may relate to density or projection effects. A number of other correlations proposed by previous workers as tests for their models were sought but not found.

Subject headings: line formation — quasars

I. INTRODUCTION

Previous detailed studies of quasar emission lines have revealed that there is a significant velocity shift between high ionization lines such as C IV 1549 (Å) and low ionization species in the same wavelength region, such as O I 1305 (Gaskell 1982; Wilkes and Carswell 1982; Wilkes 1984, 1986, 1987) amounting to ~ 1000 km s^{-1}. Wilkes also showed that there is general, but not detailed, agreement between the Lyα, N V 1240, C IV 1549, and C III] 1909 line profiles in most cases, consistent with most of the emission in these lines arising in the same region.

Work on the hydrogen emission line fluxes, following a pioneering study by Baldwin (1977), has shown that the Lyα/Hα flux ratio in quasars usually lies in the range 1–2 (see, e.g., Allen *et al.* 1982), rather than the value ~ 10 expected from case B recombination. Two possibilities have been suggested to explain the observed ratio: loss of trapped Lyα photons on dust grains in the emission region reducing the observed Lyα flux (e.g., Weedman 1986), and collisional excitation and ionization from the $n = 2$ level in X-ray heated H I regions which are optically thick to Balmer line radiation, leading to enhanced Balmer line fluxes (Kwan and Krolik 1981).

The observed velocity shift between low and high ionization lines in the ultraviolet part of the spectrum suggests a test for the X-ray heated Balmer line enhancement model. If the Balmer lines arise predominantly by this mechanism, then the Hα line, in particular, should show broad agreement with lines from O I and Mg II which also arise in H I regions. By contrast, in the dust absorption model there is no reason to expect to observe similar profiles in these lines except occasionally by chance.

With the aims of testing such models, and of probing the ionization and dynamical structure of quasar line-emission regions, we have undertaken optical and infrared spectroscopic observations of a number of high redshift, $1.3 \lesssim z \lesssim 2.4$, quasars. These have yielded profiles of a number of the stronger lines from Lyα to Hα in several objects, and a comparison between Hα and high ionization lines in a total of 18 quasars.

II. OBSERVATIONS

Observations were made of known bright quasars with redshifts such that the Hα line falls in the *H* or *K* infrared window, and which are accessible from the AAT. This led to the selection of objects with a declination $< +25°$, $z \sim 1.4$ or 2.2 and magnitude (*H* or *K*) < 15. Using known quasars biased the sample toward radio-selected objects (these accounted for $\sim 50\%$ of the sample and were mainly Parkes objects) with one object discovered by X-ray and the rest discovered by optical means. Observational details are given in Table 1.

Infrared spectra were obtained using the 16-element InSb array spectrometer (Fabry-Perot infrared grating spectrometer—FIGS; Bailey *et al.* 1988) on the Anglo-Australian

TABLE 1

OBSERVATIONS

	Optical Data			Infrared Data			
	Exposure(s)						
Object	IPCS	FORS	Date	Band	Resolution	Exposure(s)	Date
0005−239.........	2000	2000	1987 Nov 1	*H*	540	2106	1987 Nov 4
0122−380.........	2000	2000	1987 Nov 1	*K*	470	5463	1987 Nov 4
0237−233.........	668	668	1987 Feb 3	*K*	480	3721	1986 Dec 27
	2000	2000	1987 Nov 1	*K*	480	3640	1987 Nov 4
0329−385.........	2000	...	1987 Oct 31	*K*	520	3203	1987 Nov 4
	2000	2000	1987 Nov 1				
0424−131.........	2500	...	1987 Oct 31	*K*	470	5309	1987 Mar 14
	2000	2000	1987 Nov 1				
0743−673.........	2501	...	1987 Oct 31	*H*	570	5466	1987 Mar 14
	2000	2000	1987 Nov 1	*H*		2731	1987 Nov 4
	2000	2000	1988 Apr 26	*H*		5555	1988 Apr 30
0859−140.........	700	900	1987 Nov 1	*H*	510	7432	1987 Mar 15
	1951	1958	1988 Apr 26				
1011+250.........	...	...	...	*H*	590	5462	1987 Mar 15
1101−264.........	1020	1020	1987 Feb 3	*K*	480	17211	1986 Sep 5
						2730	1987 Mar 15
						11016	1987 Mar 16
				H	520	3733	1987 Mar 16
1222+228.........	2000	2000	1988 Apr 26	*K*	450	5557	1987 Mar 15
1246−057.........	1020	1020	1987 Feb 3	*K*	470	14223	1986 Sep 7
						3644	1987 Mar 14
1309−056.........	2203	2333	1988 Apr 26	*K*	470	8193	1987 Mar 15
1331+170.........	2000	2000	1988 Apr 26	*K*	460	5556	1987 Mar 16
						3308	1988 May 1
1346−036.........	2000	2000	1988 Apr 26	*H*	500	4916	1988 Apr 30
1416+067.........	2000	2000	1988 Apr 26	*H*	550	5463	1987 Mar 14
						8025	1988 Apr 30
1448−232.........	800	800	1987 Feb 3	*K*	480	7097	1986 Sep 7
						6372	1987 Mar 14
1821+107.........	2417	1800	1988 Apr 26	*H*	530	6280	1988 Apr 30
2326−477.........	2000	...	1987 Oct 31	*H*	510	7662	1988 Apr 30
	2000	2000	1987 Nov 1				

Telescope (AAT), with a resolution $R \sim 550$ in the H window and $R \sim 470$ at K. The detector elements are each 0.1 mm wide and spaced by 0.6 mm, and the grating was rapidly scanned to fill the gaps between the detectors to give a basic spectrum of more than 100 points. The main difference between the quasar spectra presented here and those published previously is that the resolution is sufficiently high that the Hα profiles cover several resolution elements.

Optical spectra were obtained at the AAT using the RGO spectrograph with the image photon counting system (IPCS) shortward of 5400 Å at a resolution $R \sim 1600$, and spectra covering 5400 Å–1 μm using the faint object red spectrograph (FORS) with a resolution $R \sim 400$. We obtained optical data for our sample during all the runs except that of 1987 March. We had hoped to obtain spectrophotometry for our objects in order to compare the line fluxes, but unfortunately, the sky conditions precluded such measurements. Hence we have used measured equivalent widths in our correlation measures rather than fluxes.

The data were reduced using standard techniques in the FIGARO package on the STARLINK Vax/780 computer at the Institute of Astronomy. The optical spectra were optimally extracted using a routine similar to that described by Horne (1986) to maximize the signal-to-noise ratio in the final results. The wavelength calibrations in all wavelength regions had rms errors less than 0.15 of a resolution element.

To extract the line profiles, the continuum level must first be determined. This was done by fitting regions of the spectrum on either side of the emission line of interest and interpolating between them. The line profiles were then obtained by subtracting this continuum estimate. These are shown in Figure 1.

In principle an intercomparison of the different line profiles in each object provides the most direct test for any possible dynamical or kinematic models of the emission-line region, but none has been developed to such a detailed level. The profiles shown in Figure 1 reveal some general trends. The overall similarity of the high ionization line profiles and Lyα, and, separately, the low ionization lines (effectively Mg II) and Hα is consistent with models where much of the Hα arises in the H I region. However, even within broad ionization classes there are significant differences in some cases. Two extreme examples are 1101−264 and 1331+170 (Fig. 1), where none of the lines is a close match to another.

A first-order parameterization of the results is to determine the redshifts of each of the emission lines and determine velocity differences between them. In this case it is not very important which of the range of possibilities we use to measure the redshift, provided that we are internally consistent. Here we have fitted (if necessary multiple) Gaussian profiles to the lines and used the component required to fit the line peak to determine the redshift. This provides a good estimate for the peak redshift, but is weighted by more points, and hence less affected by noise than a pure peak determination would be. However, for strongly asymmetric lines, such as the C IV line in

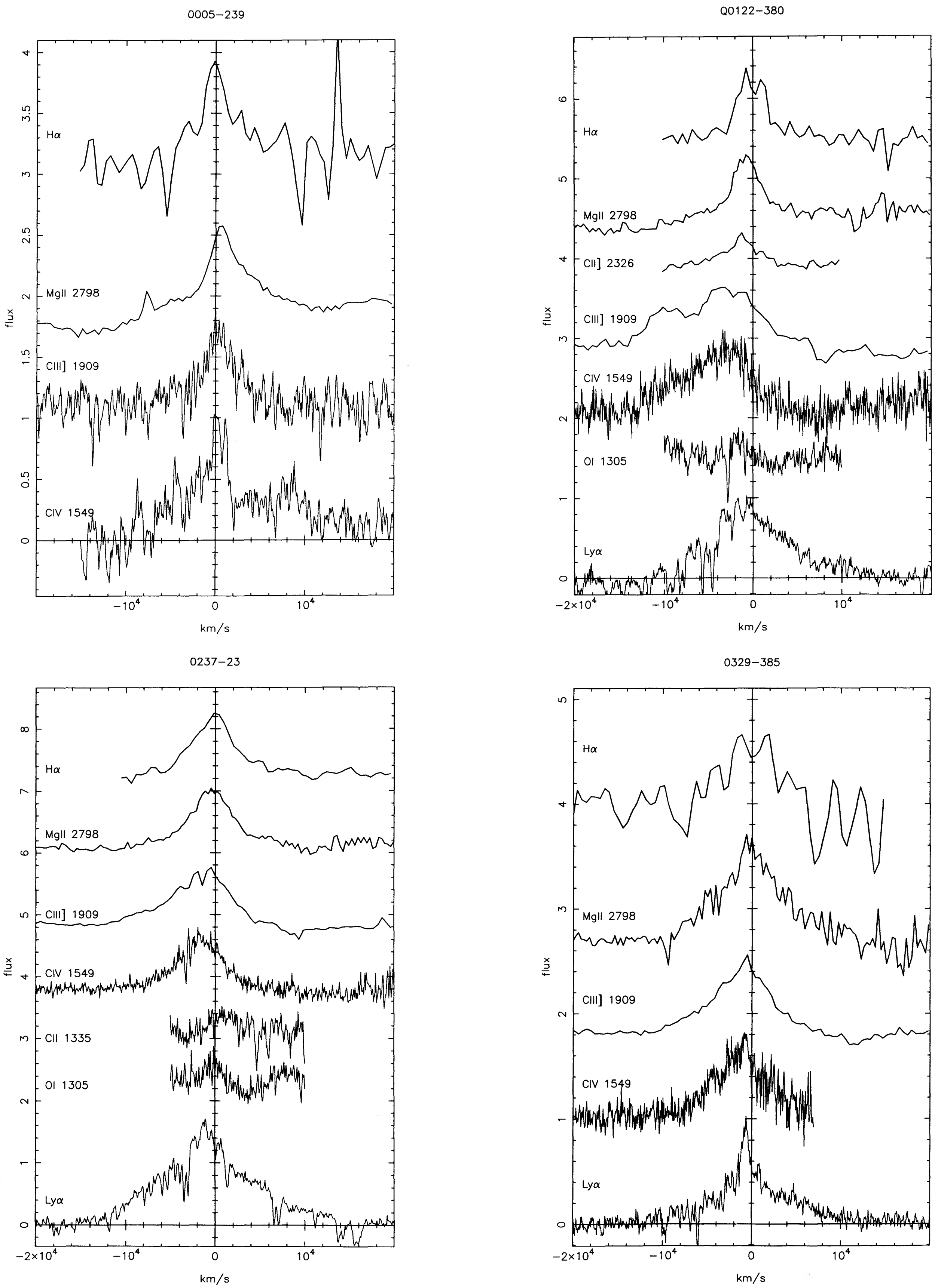

FIG. 1.—Line profiles for the quasars for which the Hα line was measured. Each has been normalized to approximately the same peak value and shifted vertically to avoid overlap. No attempt was made to remove blended components, so the Lyα profile in particular has a significant N v 1240 component. The zero velocity line is at the redshift determined for Hα.

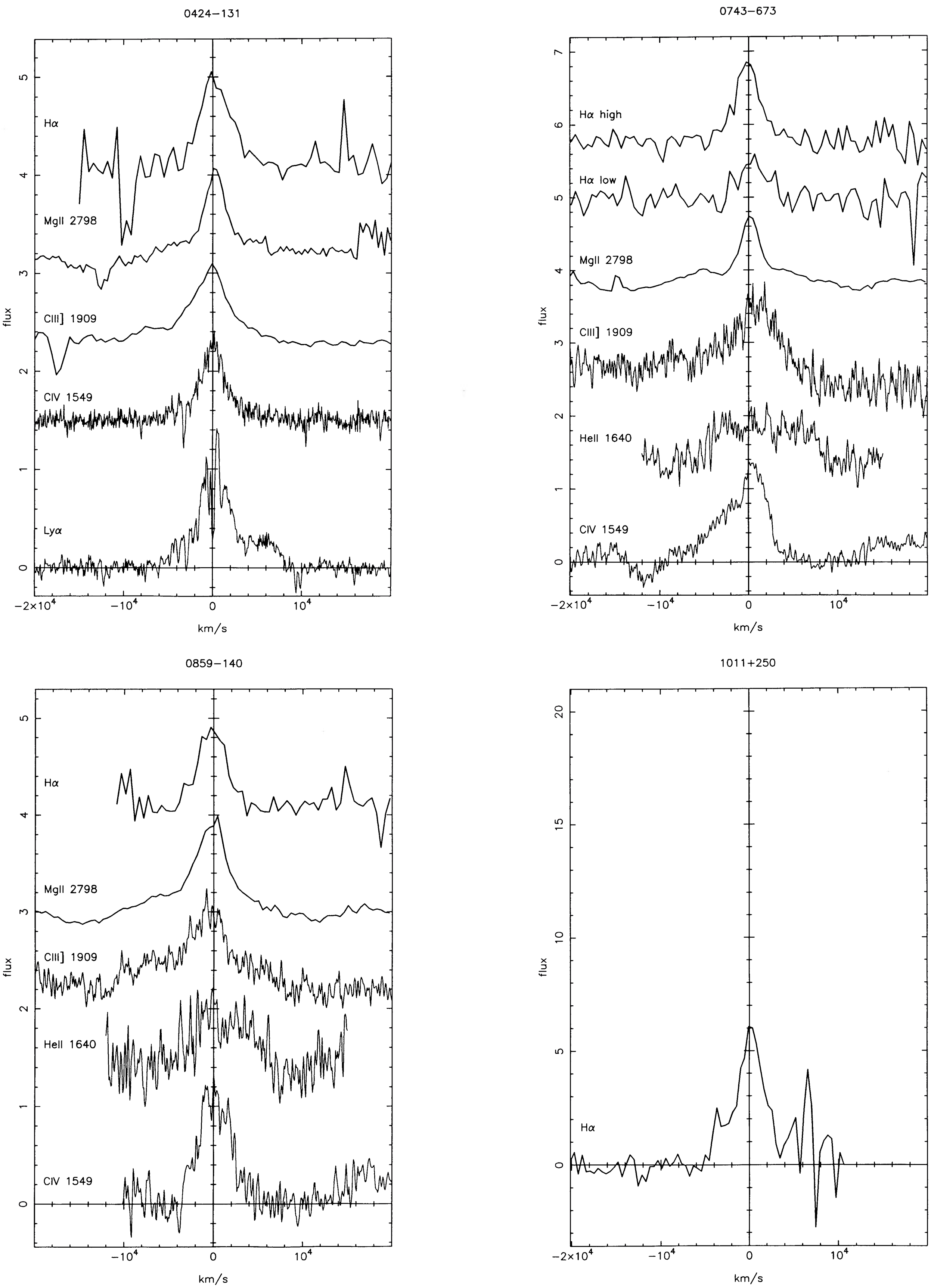

FIG. 1—*continued*

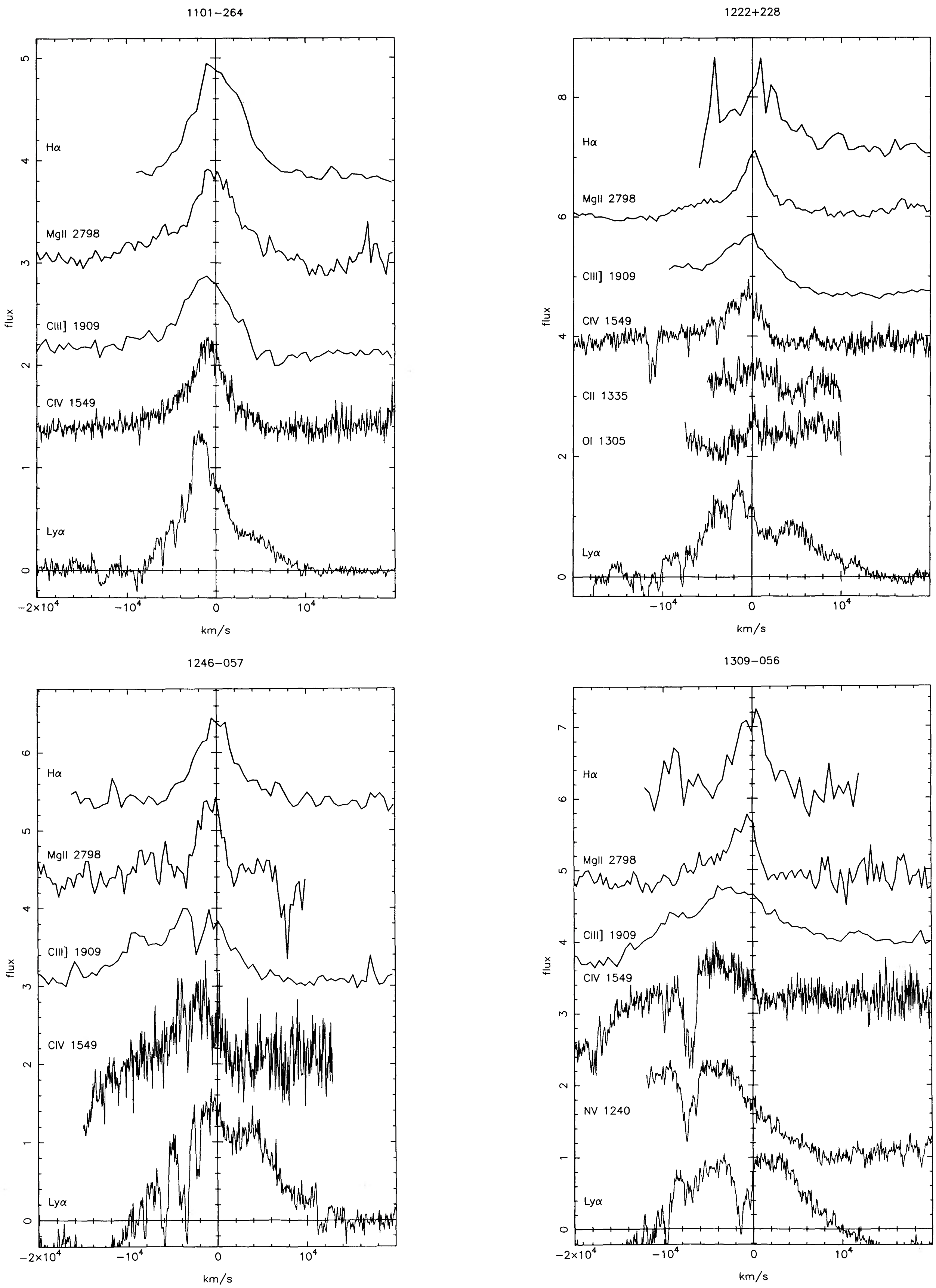

FIG. 1—*continued*

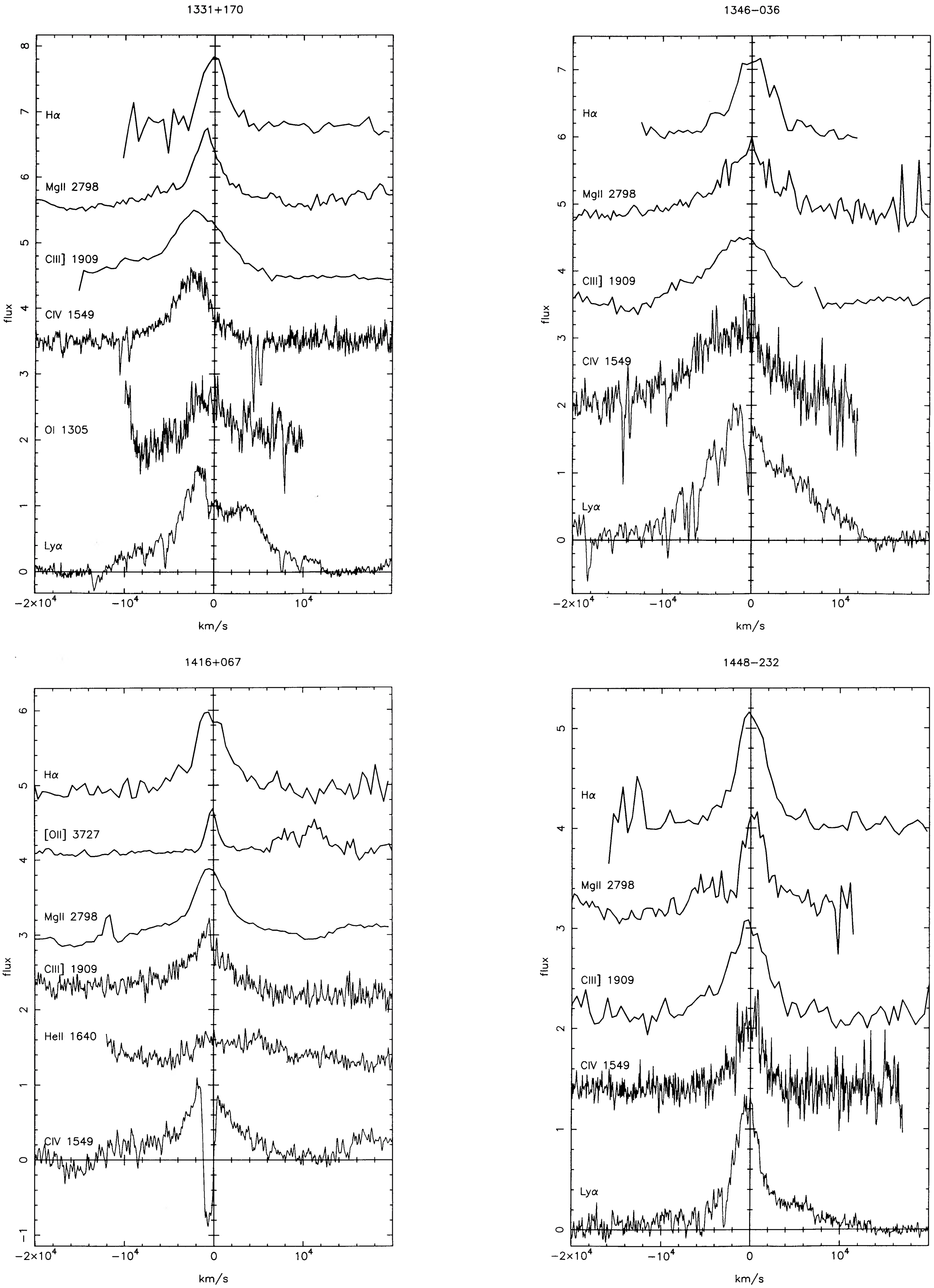

FIG. 1—*continued*

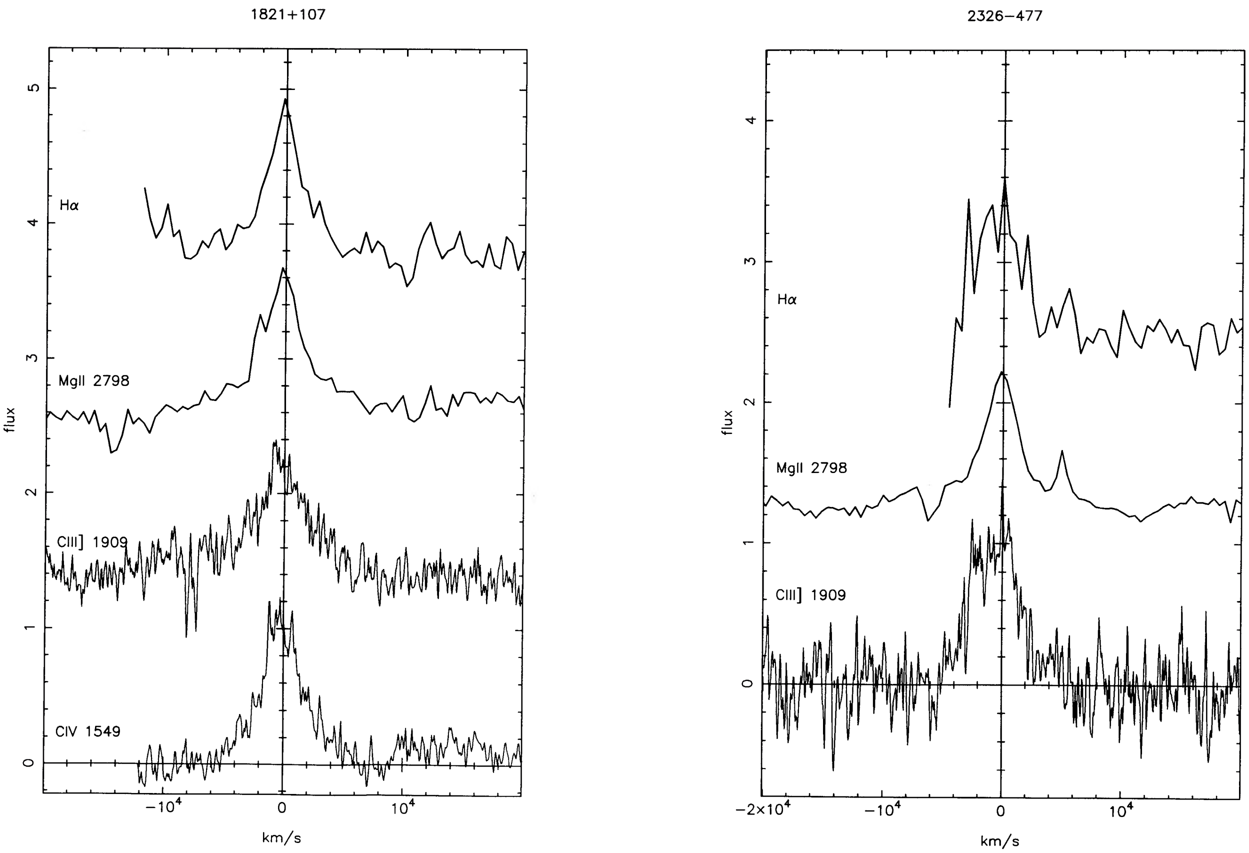

FIG. 1—*continued*

0122−380 (Fig. 1) a Gaussian fit is not possible, so a peak estimation was used. The redshifts of the lines obtained by this procedure are given in Table 2.

In all lines where absorption is present the redshifts and equivalent widths were determined by fitting regions free from obvious absorption lines in the profile. The Lyα measurements were most severely affected by absorption, and allowance was made for absorption from known or strong systems where it affected other lines. The dip in the center of the C III] 1909 profile in 1246−057, for example, is due to Mg II at $z_{\rm abs} = 1.202$. For Lyα the measurements are further complicated by blending with N V 1240, so the estimates for this line were obtained by removing those components in the fit which, by comparison with the C IV 1549 profile, are likely to arise from N V. For the other lines no attempt was made to remove blended emission components, and there are few cases where this is likely to make much difference to the results. For example, if undetected [N II] emission contributes about 10% of the flux to the Hα line the resultant additional velocity shift is only 50 km s^{-1}.

PKS 0743−673 was the only object which varied significantly during the observing program. The infrared flux in the continuum and the Hα line was ∼1.5 times higher in 1987 March than in 1987 November or 1988 April. The later two observations are rather noisy, but if anything the Hα line had an even greater redshift when it was faint than when it was bright. The value given in Table 2 is derived from the 1987 March spectrum. Unfortunately, we did not obtain an optical spectrum when it was in its "high" state in 1987 March so changes in the ultraviolet emission lines could not be observed, and the parameters for the shorter wavelength lines given in Table 2, and the profiles in Figure 1, were determined from observations made when the object was fainter. Figure 1 shows the Hα profiles separately for the "high" and the "low" states, normalized to the same flux level.

The main result from the observations of 18 quasars, that the Hα line is, on average, at ∼1000 km s^{-1} higher redshift than C IV 1549, is evident from Table 2 and shown more explicitly in Table 3. Thus the velocity shift for Hα is comparable with that found for low ionization lines by Wilkes (1987). Clearly, from Tables 2 and 3, the high ionization lines (C IV and C III]) and Lyα tend to have lower redshifts than the low ionization lines (O I and Mg II) and Hα, but there is not always good agreement within the broad ionization class. The line profiles reflect this rough similarity within the two classes. The exception to this is C III] 1909 which is often broader than the other lines. However, C III] 1909 may well be blended with Al III 1860 and Si III] 1892 (Baldwin *et al.* 1988); the width estimate applies to the whole blend and so will not be directly comparable with other line widths. Indeed, an extra component is often found in this line ∼8000 km s^{-1} shortward of the peak wavelength, consistent with a strong Al III component (e.g., in 0122−380 and 1246−057). There is a tendency for the low ionization lines to be narrower, confirming earlier results (Wilkes 1986, and references therein), though the line widths are not necessarily very different even when the velocity shift is large. The most extreme velocity shifts are found for the two broad absorption line quasars, 1246−057 and 1309−056. Here there is some uncertainty in that the high ionization lines may be affected by overlying absorption, though these two objects are

TABLE 2

MEASURED LINE PARAMETERS

Object	Lyα	O I 1304	C IV 1549			C III] 1909			Mg II 2798			Hα			
	z	z	z	EW[a]	Width	z	EW	Width	z	EW	Width	z	EW	Width	L(Hα)[b]
0005−239			1.411	49.5:	2000:	1.409	11.4	3600	1.413	19.2	3200	1.407:	369	3000:	45.17
0122−380	2.185:	2.189	2.178:	17.4	9000	2.189	47.2	12000:	2.199	19.2	3381	2.207	259	3900	45.50
0237−233	2.226	2.246	2.215	19.8	5600	2.236	22.0	7200	2.231	25.8	5300	2.236	281	4600	46.05
0329−385	2.435	2.45::	2.433	48.8	6000:	2.437	22.0	6300	2.437	35.0	8000:	2.443	150::	...	45.4::
0424−131	2.153		2.165	31.2	2700	2.162	19.0	4300	2.167	10.4	2800	2.163	356	4100	45.74
0743−673			1.511	23.8	5100:	1.509	19.5	6000:	1.513	12.5	2700	1.511	231	2900	45.45
0859−140			1.336	19.5	5600	1.337	24.5	5000	1.340	35.2	4500	1.341	225	3900	45.18
1011+250			1.631[c]	41.0								1.637	232	3200	46.10
1101−264	2.133		2.143	29.9	4400	2.141	44.4:	6200:	2.151	23.0	5400	2.152	325	6700	46.18
1222+228	2.045	2.057	2.047	10.4	4400	2.053	10.4	...	2.056	17.2	2800	2.062:	270:	3500:	45.91
1246−057	2.227:		2.219	9.9	5200	2.211	19.6	10500:	2.238	7.5	3200:	2.246	244	4700	46.99
1309−056	2.183	2.202::	2.194	9.0	6500	2.209	28.5	12000	2.234	16.5	3700	2.239	150	3900	46.20
1331+170	2.084	2.100	2.083	19.3	4500	2.086	21.7	6600	2.096	15.9	3200	2.103	140	3200	45.78
1346−036	2.343		2.352:	18.6:	9700:	2.351	15.6	5700	2.368:	30.3:	4500:	2.367	238	5200	45.87
1416+067			1.438	40.5	3400:	1.438	24.0	4200	1.439	23.7	4300	1.442	326	4100	45.30
1448−232	2.214		2.216	20.4	3800	2.213	55.9	4800	2.223	19.1	2900	2.218	412	3700	46.02
1821+107			1.362	34.0	3700	1.360	17.8:	4300	1.363	19.9	4000	1.364	274	3500	45.30
2326−477						1.304	12.9	5100	1.306	19.1	3400	1.305	216	5000::	45.3::

NOTE.—The redshift error is typically $\Delta z \sim 0.001$, with larger errors for Lyα because of the presence of N V 1240 and sharp absorption lines and O I 1304 because, when present, it is weak.

[a] Rest equivalent widths are in Å, and the line widths are full width half-maxima in km s^{-1}.

[b] L(Hα) is given in log (ergs s^{-1}) for a universe with $H_0 = 50$ km s^{-1} Mpc^{-1} and $q_0 = 0$.

[c] C IV data from Young *et al.* 1982.

noteworthy in that their broad absorption systems are detached—i.e., the emission lines do not appear to be strongly absorbed.

III. INTERPRETATION

The existence of velocity shifts between different lines is not compatible with single-zone models for the quasar broad emission-line region (e.g., Kwan and Krolik 1981). Doubts have already been raised on this issue from previous studies of this sort (e.g., Gaskell 1982; Wilkes 1984, 1986) and detailed model calculations predicting the intensities of both the low- and high-ionization lines in a single-zone model (e.g., Davidson 1977; Collin-Souffrin, Dumont, and Tully 1982; Collin-Souffrin 1986). Since the shift is systematic, it must be that there are mass flows in the line-emitting gas and some obscuration of part of the flow. A further consequence of the general agreement between the Hα and low ionization lines rather than the high ionization lines and Lyα is that the bulk of the Hα observed is likely to originate in the same region which gives rise to the low ionization lines. This is consistent with models where the Balmer line emission is enhanced by collisional effects from the $n = 2$ level in hydrogen in warm H I regions (e.g., Kwan and Krolik 1981), but the profile differences indicate that the Lyα/Hα flux ratio from this region must be even smaller than had been supposed. Profile comparisons with PKS 0237−23, for example, suggest that for the material

TABLE 3

VELOCITIES RELATIVE TO Hα (km s^{-1})

Object	Lyα	O I 1305	C IV 1549	C III] 1909	Mg II 2798
0005−239			500	200	1200
0122−380	2100	−1700	−2700	−1700	−700
0237−233	−900	900	−2000	0	−500
0329−383	700		−900	−500	−500
0424−131	900		200	−100	400
0743−673			0	−200	200
0859−140			−600	−500	−100
1011+250			−700		
1101−264	−1800		−900	−1000	−100
1222+228	−1700	−500	−1500		−600
1246−057	−1800		−2500	−3300	−700
1309−056	−5200	(−3400)	−4200	−2200	−500
1331+170	−1800	−300	−1900	−1700	−700
1346−036	−2100		−1300	−1400	100
1416+067			−500	−500	−400
1448−232	−400		−200	−500	500
1821+107			−300	−500	−100
2326−477				−100	100
Mean	−1770	−390	−1140	−880	−140
σ	1230	930	1180	920	510

producing most of the Hα, Lyα/Hα $\lesssim 0.9$, which is ~ 2 times smaller than the value quoted by Allen *et al.* (1982) using the total fluxes in each line.

In constraining such models it is clearly important to know which of the line redshifts is an indicator of the true redshift, i.e., the redshift of the galaxy in which the quasar presumably lies. An obvious way to determine this to sufficient accuracy is to measure the redshifts of any narrow forbidden lines, particularly [O III] 4959, 5007, or [O II] 3727. [O II] 3727 is present in 1416+067, but unfortunately this is a case where there is no significant velocity shift between the low and high ionization lines. [O I] 6300 may be present in the spectrum of 1246−057 at a redshift consistent with that of the Hα line, but the feature may be no more than a noise spike. An attempt was made to measure the [O III] lines and Hβ in 1101−264, but the lines were not detectable. Thus we have to resort to indirect arguments.

Gaskell (1982) noted that the Balmer line and forbidden line redshifts are generally similar in low-redshift quasars and Seyfert galaxies, so, if high-redshift quasars behave in the same way, this leads to the conclusion that the Hα and low ionization lines define the redshift. Then the high ionization lines would be seen blueshifted with respect to the object. Under these circumstances heavy element absorption systems seen in quasar spectra at redshifts up to ~ 3000 km s^{-1} greater than the Lyα and C IV emission redshift (e.g., Weymann *et al.* 1977) would be likely to have smaller velocities with respect to the quasar. Thus the inferred velocity dispersion in the cluster containing the quasar could be reduced to values compatible with present-day clusters of galaxies.

However, this argument is not conclusive. Recent work by L. Bryant and M. J. Ward (in preparation) using *IUE* spectra of low-redshift quasars and active galaxies shows that the velocity shifts between Lyα and Hβ are somewhat smaller than for the quasars we have observed, so the link between high- and low-redshift objects is not clear. Junkkarinen (1988) has described observations of some quasars where the velocity shifts are smaller than those we have found, and presents evidence that the forbidden line redshift generally agrees with that of the C IV 1549 line. Also, it is notable that the Lyα forest absorption in high-redshift quasars terminates very close to the peak of the Lyα emission. This would indicate that either the high ionization line redshift is the correct one, or that there is some coincidence between the internal velocity shift in the quasar and the velocity in the Hubble flow local to the quasar to which its ionizing influence extends (see Bajtlik, Duncan, and Ostriker 1988 for a discussion of the quasar ionization of the Lyα clouds). However, this point has yet to be investigated in any detail, so the balance of the evidence favors the low ionization lines as indicating the redshift of the object.

A currently favored model (e.g., Collin-Souffrin *et al.* 1988) is that of an optically thick accretion disk giving rise to the greater part of the low-ionization line emission (e.g., Hα, Mg II), and an optically thin system of clouds about this disk giving rise to the high ionization lines (e.g., Lyα, C IV). One might expect that the consequences of this model might be seen in the resulting line profiles, especially if the optically thin material is flowing in or out and if the accretion disk occults some of this material. For example, Netzer (1985) has suggested that a correlation should exist between the rest equivalent width of the C IV line and the inclination of the disk in the emitting clouds/accretion disk model. We would expect the velocity shift to depend on the inclination also, with a maximum shift for face-on systems, so, if this picture is correct, we would expect a trend between C IV equivalent width and velocity shift. This is shown in Figure 2, where it can be seen that there may be a weak correlation. However, a similar study by including data from a larger, albeit lower, resolution sample (Wilkes 1984) does not show this effect.

Such correlations may be masked, however, by the scattering medium required to account for the amount of energy reaching the outer parts of an accretion disk in order to generate the low-ionization line intensities. Kallman and Krolik (1986) showed that electron scattering can yield a nearly sym-

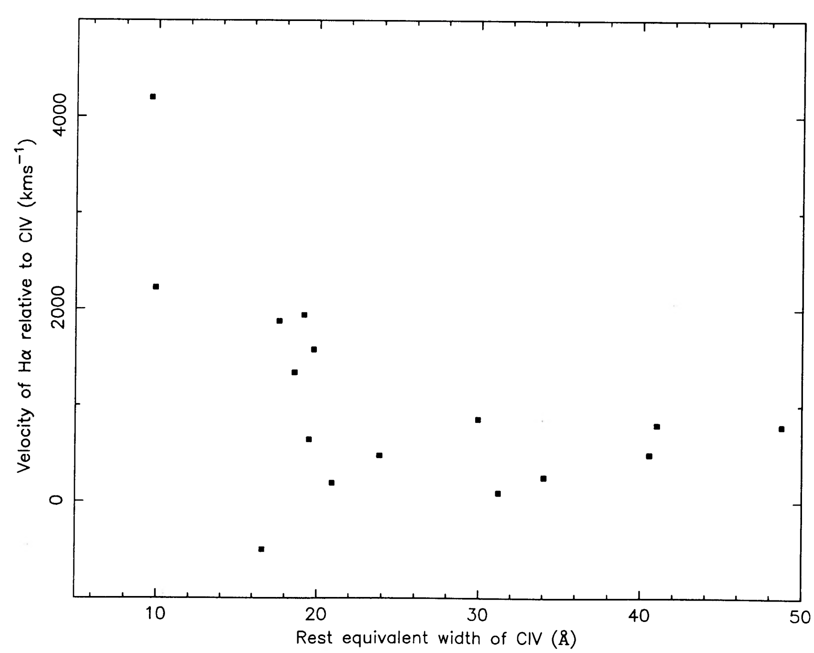

FIG. 2.—The velocity difference between Hα and C IV 1549 vs. the equivalent width of the C IV 1549 line

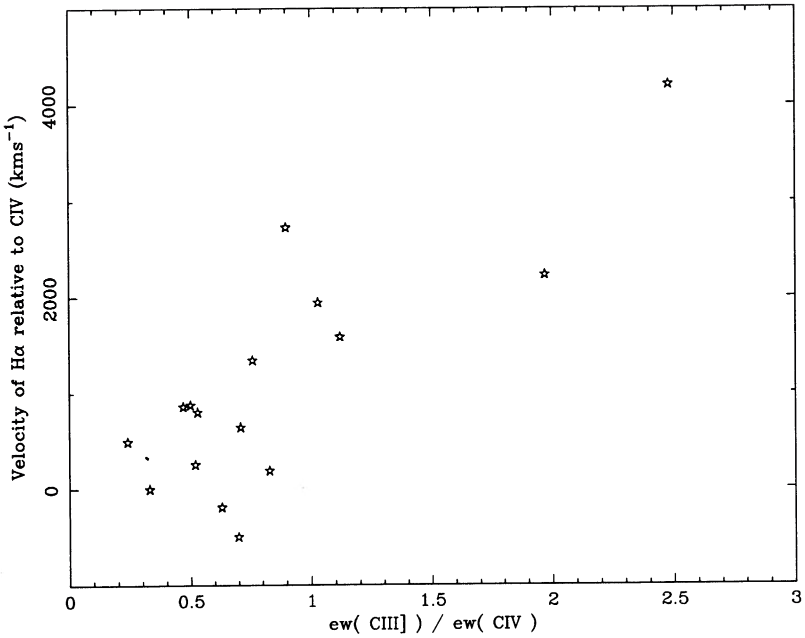

FIG. 3.—The Hα–C IV 1549 velocity difference vs. the equivalent width ratio of C III] 1909 to C IV 1549

metric line profile with a shifted peak, the peak being blueshifted for infall and redshifted for outflow. The maximum velocity shift predicted between the high and low ionization lines is roughly equivalent to the HWHM value of the C IV line, though the result is strongly model-dependent. This value provides a reasonable estimate of all the velocity shifts observed here except those in 1309−056. However, the assumptions of this model may not be realistic enough to reflect the true conditions in the objects studied here (for instance, the scattering medium is denser than that postulated by Collin-Souffrin *et al.* 1988). Whether shifted, symmetric profiles are possible in a less-dense medium remains an open question until the appropriate model calculations are done.

An alternative explanation has been suggested by Ferland (1987), who proposed that selective absorption arising from the inner region of an accretion disk could cause an apparent blueshift in the opacity sensitive high ionization lines. However, the small number of objects which have an observed Lyman limit absorption associated with the emission line region (Baldwin and Smith 1983) poses a problem for this model.

We also sought correlations between velocity shift and line width as an indicator of possible aspect and obscuration effects, but no trends were found. Nor was there any apparent correlation of the velocity shift with radio properties, X-ray emission, spectral index, or Lyα/Hα flux ratio. A possible correlation exists between the velocity shift and the ratio of EW(C III])/EW(C IV) (Fig. 3). The interpretation of this is far from clear. It may be a luminosity effect (the Baldwin effect observed in the equivalent width of the C IV line), or a density effect (see, for example, Mushotzky and Ferland 1982). If the effect is real and related to density, this would suggest that low-density clouds are accelerated to higher velocity than high-density clouds, as might be expected intuitively.

IV. CONCLUSIONS

The Hα emission lines in high redshift quasars have broadly similar redshifts to low ionization lines from O I and Mg II, and these are redshifted by $\sim$1000 km s^{-1} with respect to higher ionization lines. Thus it appears that most of the Hα emission we see comes from H I regions near the quasar, and so is consistent with models in which it arises through collisional excitation and ionization from the $n = 2$ level in hydrogen in this region. These results also reinforce earlier work (Wilkes 1987 and reference therein) on velocity shifts between species, and the need for at least a two-zone model for quasar emission lines involving mass flows and internal obscuration.

The velocity shift may be explained in a number of ways, but in most cases there are consequences for other line parameters which should give rise to a correlation between the velocity difference and some other observable quantity. We have found that the highest velocity differences are associated with broad absorption line objects, and there is probably a correlation between the velocity shift and the C III]/C IV equivalent width ratio. The explanation for either of these is unknown.

We are grateful to the staff of the Anglo-Australian Observatory, without whose assistance the observations reported here would not have been possible. B. R. E. acknowledges financial support from the SERC through a research studentship.

REFERENCES

Allen, D. A., Barton, J., Gillingham, P., and Carswell, R. F. 1982, *M.N.R.A.S.*, **200**, 271.
Bailey, J., *et al.* 1988, *Pub. A.S.P.*, **100**, 1178.
Bajtlik, S., Duncan, R. C., and Ostriker, J. P. 1988, *Ap. J.*, **327**, 570.
Baldwin, J. A. 1977, *M.N.R.A.S.*, **178**, 67P.
Baldwin, J. A., McMahon, R., Hazard, C., and Williams, R. E. 1988, *Ap. J.*, **327**, 103.
Baldwin, J. A., and Smith, M. G. 1983, *M.N.R.A.S.*, **204**, 331.
Collin-Souffrin, S. 1986, *Astr. Ap.*, **166**, 115.
Collin-Souffrin, S., Dumont, S., and Tully, J. 1982, *Astr. Ap.*, **106**, 302.
Collin-Souffrin, S., Dyson, J. E., McDowell, J. C., and Perry, J. J. 1988, *M.N.R.A.S.*, **232**, 539.
Davidson, K. 1977, *Ap. J.*, **218**, 20.
Ferland, G. J. 1987, in *Emission Lines in Active Galactic Nuclei*, ed. P. M. Gondhalekar Rutherford Appleton Laboratory Publication, RAL-87-109, p. 107.

Gaskell, C. M. 1982, *Ap. J.*, **263**, 483.
Horne, K. 1986, *Pub. A.S.P.*, **98**, 609.
Junkkarinen, V. T. 1988, in *IAU Symposium 134, Active Galactic Nuclei*, in press.
Kallman, T. R., and Krolik, J. H. 1988, *Ap. J.*, **308**, 805.
Kwan, J., and Krolik, J. H. 1981, *Ap. J.*, **250**, 478.
Mushotzky, R. F., and Ferland, G. J. 1982, *Ap. J.*, **278**, 558.
Netzer, H. 1985, *M.N.R.A.S.*, **216**, 63.
Weedman, D. W. 1986, *Quasars* (Cambridge: Cambridge University Press).
Weymann, R. J., Williams, R. E., Beaver, E. A., and Miller, J. S. 1977, *Ap. J.*, **213**, 619.
Wilkes, B. J. 1984, *M.N.R.A.S.*, **207**, 73.
———. 1986, *M.N.R.A.S.*, **218**, 331.
———. 1987, in *Emission Lines in Active Galactic Nuclei*, ed. P. M. Gondhalekar Rutherford Appleton Laboratory, RAL-87-109, p. 79.
Wilkes, B. J., and Carswell, R. F. 1982, *M.N.R.A.S.*, **201**, 645.
Young, P. J., Sargent, W. L. W., and Boksenberg, A. 1982, *Ap. J. Suppl.*, **48**, 455.

J. A. Bailey and M. G. Smith: Joint Astronomy Centre, 665 Komohana Street, Hilo, HI 96720

R. F. Carswell, B. R. Espey, and M. J. Ward: Institute of Astronomy, Madingley Road, Cambridge CB3 0HA, England